Available online at www.sciencedirect.com
ScienceDirect
Journal of the European Ceramic Society 30 (2010) 171–176
www.elsevier.com/locate/jeurceramsoc

Preparation of concentrated barium titanate suspensions incorporating nano-sized powders

Gang Liu, Dou Zhang, Tim W. Button *

School of Metallurgy and Materials, University of Birmingham, Edgbaston, Birmingham B15 2TT, UK

Available online 9 July 2009

Abstract

In order to reduce agglomeration and overcome the low packing density issues of working with nano-sized powders, a colloidal processing route has been chosen in this study. Commercial $BaTiO_3$ (BT) powders with a particle size in the range of 50 nm have been dispersed in the aqueous media. Rheological properties have been analyzed on suspensions with different solids loading, dispersant concentration, and pH conditions. Optimum dispersing conditions were obtained for suspensions prepared at basic pH (pH 10) with 0.646 wt% ammonium poly (acrylic acid) (NH_4PAA) as a dispersant. Suspensions have been centrifugally cast to obtain the green body, and the sintering conditions have been investigated by examining the phase evolution, microstructures and electrical properties of the sintered samples through XRD, SEM and dielectric measurements, respectively. The results show that for a 45 vol% suspension sintered at 1325 °C, the density of bulk ceramic can reach 5.85 g/cm^3, nearly 97.0% of the theoretical density.

Keywords: Nano-size; $BaTiO_3$; Suspension; Centrifugal cast; Sintering

1. Introduction

$BaTiO_3$ (BT) is an important ceramic material in the electronics industry. It has been widely used to fabricate high-value capacitors,[1,2] thermistors,[3,4] and piezoelectric sensors.[5,6] The final electrical properties of BT devices are dependent on the microstructural characteristics. An accurate microstructural control is essential when specific electrical requirements have to be fulfilled. However, the manufacturing process plays a key role in the control of microstructural characteristics. Among the commercial consolidation techniques, colloidal processing can provide a homogeneous microstructure in the devices, which allow better quality control.[7] Colloidal processing consists of the preparation of slurries by mixing the ceramic powder, a solvent and an organic agent used as dispersant. Generally, colloidally stable suspensions are preferred, since they usually produce higher average packing densities than flocculated suspensions. However, the interaction between the powder, the solvent and the organic agent can be rather complicated. The significance of a well-dispersed suspension to optimize the fabrication of electronic device has motivated many studies of colloidal stability of BT both in aqueous[8–16] and non-aqueous media.[17–19] Due to minimal environmental impact, aqueous processing is an attractive option for future development, though manufacturers still prefer non-aqueous processing. Recently, nano-sized powders have attracted much attention in order to gain significant improvement in key properties. In case of BT, improved performance such as the potential for device miniaturization, and improved dielectric properties, can be achieved by incorporating nano-sized BT powders.[20–22] Much research concerning colloidal processing in aqueous media has been done,[8–15] however, to our knowledge, only a few investigations about colloidal processing with nano-sized BT powders in aqueous media[16,23] have been found. Therefore, there is a need to study in the colloidal processing using nano-sized BT powders in aqueous media.

Moreover, the colloidal processing is a versatile route, because following on the suspension preparation, many forming techniques can be utilized, including slip casting, tape casting, and screen printing, together with centrifugal casting as a simple and high efficient route.[24,25]

In this paper, the preparation of aqueous BT suspensions with high solids content and viscosities suitable for centrifugal casting has been investigated.

* Corresponding author.
E-mail addresses: GXL747@BHAM.AC.UK (G. Liu), t.w.button@bham.ac.uk (T.W. Button).

0955-2219/$ – see front matter © 2009 Elsevier Ltd. All rights reserved.
doi:10.1016/j.jeurceramsoc.2009.06.009

2. Experimental

2.1. Materials

The commercial nano-sized BT powder (HPB-1000 (50 nm), TPL Inc., USA) was used for all experiments. Distilled water (17 MΩ cm) was used as a vehicle in this study. A small amount of ammonium polyacrylate (NH_4PAA) solution (D3021, Allied Colloids, Bradford, UK, a 40% concentrated solution of average molecular weight 3500 g/mol) was used in order to obtain stable BT slurries with high solids loading. The amount of the NH_4PAA used here is expressed as a dry weight of the powder basis (dwb), equivalent to the w/w basis of the BT powder. NH_4PAA was chosen in this study to disperse nano-sized BT powders because this dispersant is one of the most often used in aqueous solutions and its temperature of thermal decomposition by depolymerization is below 400 °C, allowing clean burnout with little residual carbon. 3 wt% B-1000 and 2 wt% B-1007 (acrylic polymer emulsion, Duramax) were added into the suspension as binder. 1 M HCl and concentrated (35%) NH_4OH were utilized to modify the pH value.

2.2. Processing

The BT suspensions were prepared by mixing powder, distilled water and dispersant under constant stirring. Slurries were ball-milled for 24 h with zirconia balls and de-aired in a vacuum desiccator. Typical batch size was 50 g. Before casting, binders were added to the suspensions, followed by ball milling at very low speed for 20 min.

BT suspensions were prepared at 30, 35, 40, and 45 vol% to characterize the effect of solids loading on viscosity, sintered density, and microstructure. The slurries were poured into soft moulds (ϕ 12 mm × H 13.5 mm),[26] which were then placed in a Clandon T-52 bench top centrifuge for half an hour at 3000 rpm. The green bodies were kept in the mould and left in the room temperature for 24 h, and then were put in an oven at 40 °C for another 24 h to dry out the water. Finally, the dried green bodies were carefully peeled off from the mould prior to sintering.

The green bodies were sintered in an air furnace at a constant heating rate of 1 °C/min to 500 °C, followed by 5 °C/min to maximum temperatures 1300, 1325, 1350, and 1400 °C for 1.5 h, respectively. After sintering, all samples were cut into discs (2 mm in thickness) for dielectric measurement. Electrodes on both sides of all BT discs were formed by sputtering Au coating.

2.3. Characterization

The rheologies of the suspensions were investigated by using the a Rheometer (Carri-med 115/A) with the cone and plane system (Truncation: 59 μm; Core: 4 cm, 20°) at the temperature of 20 °C. Crystallographic and phase analyses for the BT powder and sintered samples were performed using an X-ray diffractometer (Philips X'pert) with monochromatic Cu Kα radiation. The detection normally ranges from 10° to 80° with a step size of 0.02° and a speed of 1.2°/min. Identification of crystalline phase was carried out by comparison of XRD pattern with JCPDS standards. The sintered density of bulk BT was determined by Archimedes' method. The dielectric properties were measured at room temperature by a HP-4194A impedance analyzer. The microstructures of the samples were analyzed by scanning electron microscopy (SEM) (JSM 7000, Jeol, Tokyo, Japan)

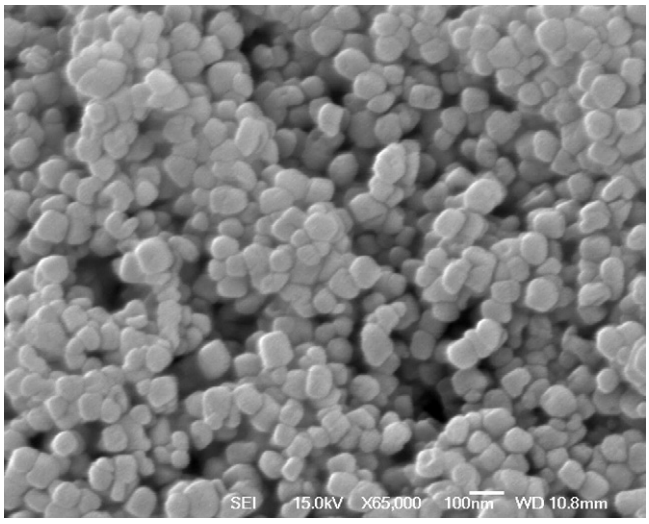

Fig. 1. SEM photo of the nano-sized BT powder.

3. Results and discussion

3.1. Powder characterization

A SEM micrograph of the BT powder used in this study is shown in Fig. 1 and the powder has a near-spherical morphology with a primary particle size around 50 nm. Fig. 2 shows the results of XRD analysis of the nano-sized BT powder. By comparing XRD pattern with JCPDS standards, the diffraction peaks from the nanoparticles can be indexed as cubic BT, as no peak splitting is observed at (2 0 0). However, impurity was found in the BT powder. The peak in the XRD pattern around

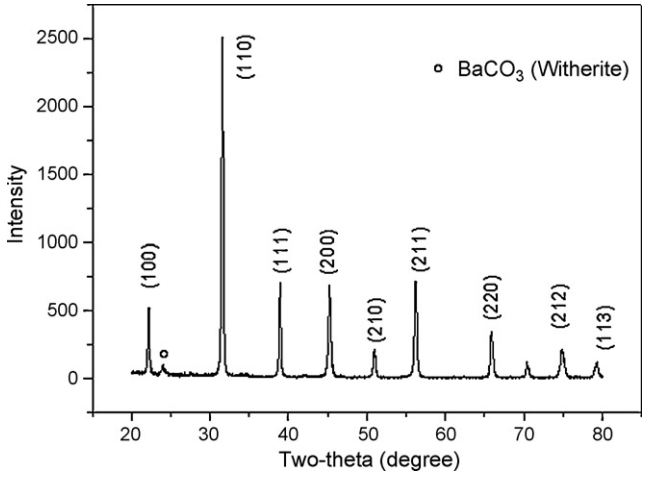

Fig. 2. XRD patterns for nano-sized BT powder.

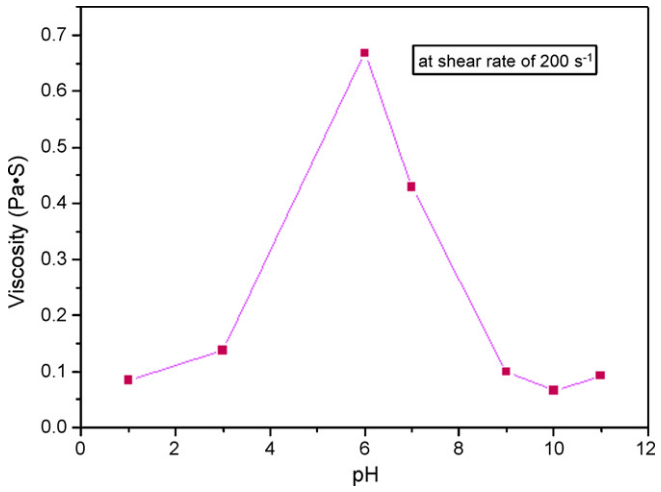

Fig. 3. Viscosity versus pH for the 30 vol%, 0.646 wt% NH_4PAA BT suspension.

$2\theta = 24^\circ$ indicates the existance of $BaCO_3$ in the BT powder. The tetragonality (c/a ratio) of this nano-sized BT powder is 1.0 caculated from the XRD crystal lattice parameters. The Ba/Ti molar ratio is 0.995–1.010, which is provided by the BT powder manufacturer.

3.2. *Rheology properties of $BaTiO_3$ suspensions*

The variation of the viscosity of a 30 vol% BT suspension with 0.646 wt% NH_4PAA by adjusting the pH value is shown in Fig. 3. The natural pH of the suspension was around 10. NH_4PAA, a polyelectrolyte, was used to provide the electrosteric stabilization energy to the ceramic powders in suspension. When changing the pH value of the suspension, both the ionisation of NH_4PAA absorbed on the surface of the particles and the structure of the double-electrical layer will be affected. Therefore, the electrostatic repulsion energy will be changed. Meanwhile, the steric stabilization can also be influenced by the pH value. As shown in Fig. 3, with decreasing the pH from the intrinsic pH value, the viscosity of the suspension first increased, and then decreased. The maximum viscosity occurred at a pH value around 6, which is consistent with the isoelectric point (IEP) of BT in López's work.[12] When the pH value was continuously increased from the intrinsic value, the viscosity increased as

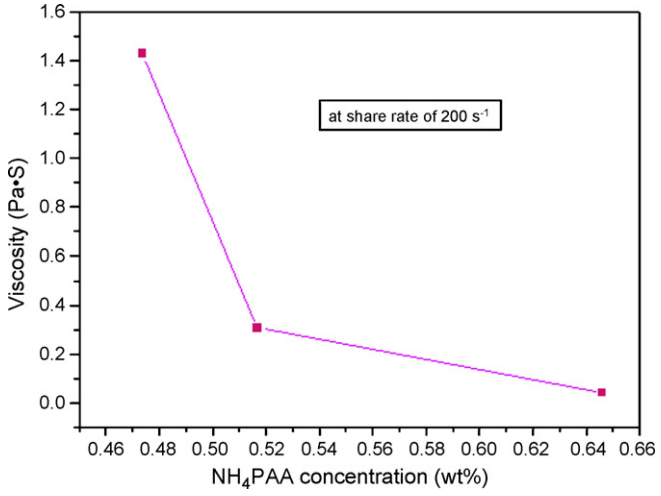

Fig. 4. Viscosity versus NH_4PAA concentration for 30 vol% BT suspension at share rate of 200 S^{-1}.

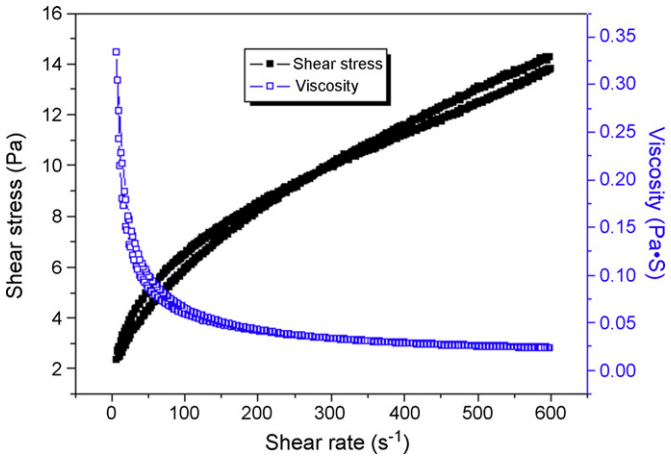

Fig. 5. Typical rheological flow behaviour of 30 vol% BT suspension with 0.646 wt% NH_4PAA.

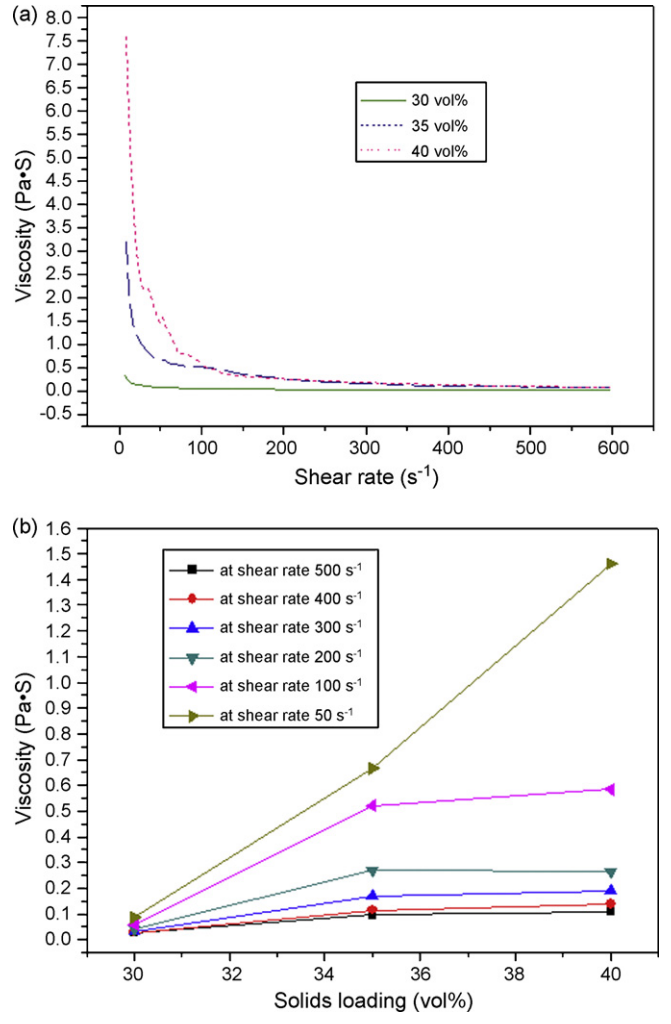

Fig. 6. (a) Flow behaviour of BT suspensions with 0.646 wt% NH_4PAA of different solids loading. (b) Viscosity of BT suspensions containing 0.646 wt% NH_4PAA of different solids loading at different shear rate.

well. Therefore, for further study, there is no need to modify pH value of the suspension to obtain good liquidity since the viscosity of the suspension at the natural pH is suitable for processing. The change of the viscosity of the 30 vol% BT suspension with NH_4PAA concentration is displayed in Fig. 4. In the experimental range, the viscosity of the suspension decreased dramatically as the NH_4PAA concentration increased.

The relationship between the shear rate and shear stress, as well as between the viscosity and the shear rate of 30 vol% BT suspension with 0.646 wt% NH_4PAA, is shown in Fig. 5. A relatively steady decrease of the viscosity with increasing the shear rate was observed and shown in Fig. 6, indicative of a well-dispersed suspension. The viscosities of BT suspension with a typical shear thinning characteristic with different solids content suspensions are shown in Fig. 6. When the solids loading is more than 40 vol%, the viscosity increased dramatically, and the suspension with a solids loading of 45 vol% could not be tested. As shown in Fig. 6, the higher the solids content, the more viscous the suspension becomes. The viscosity curves of 35 and 40 vol% present typical shear thinning or pseudoplastic curves. Normally it is convenient to process under shear thinning conditions because at low shear rates the viscosity of the slurry is high enough to delay sedimentation, whilst at high shear rates the viscosity is low enough to produce a castable state.

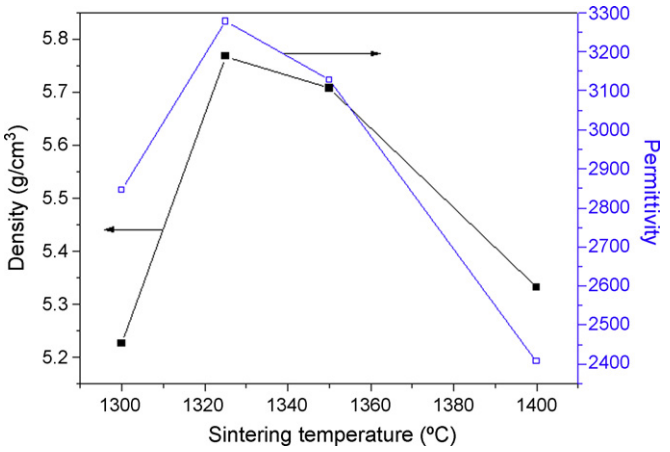

Fig. 7. Density and room temperature relative permittivity as a function of sintering temperature for 30 vol% BT with 0.646 wt% NH_4PAA.

3.3. Characteristic of centrifugally cast bulk $BaTiO_3$ ceramics

To optimize the sintering condition, four different sintering temperatures were tested and their effects on the density and relative permittivity of the bulk BT ceramics from a 30 vol% suspension with 0.646 wt% NH_4PAA are shown in Fig. 7. As

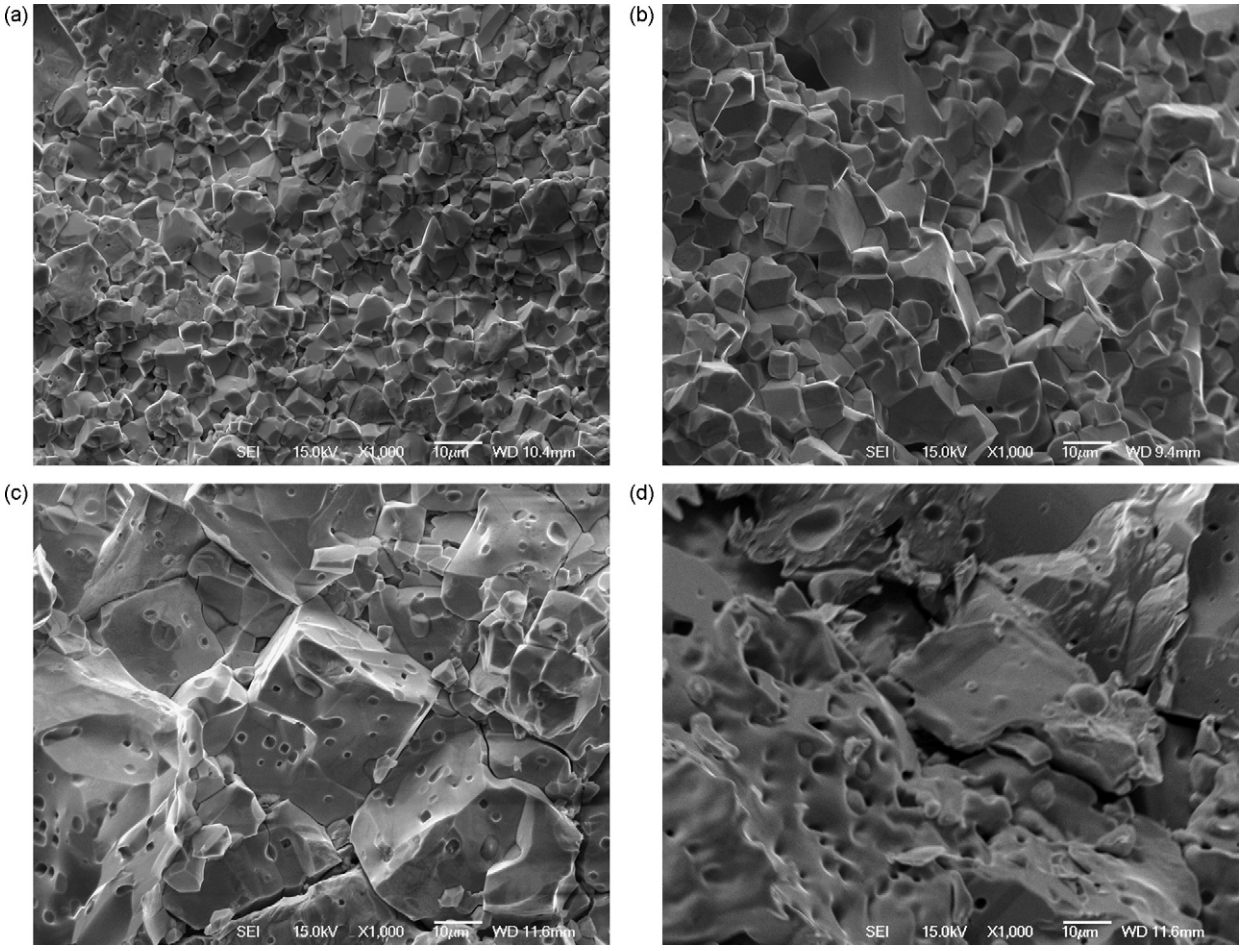

Fig. 8. Cross-section of 30 vol% sintered samples (0.646 wt% NH_4PAA): (a) 1300, (b) 1325, (c) 1350, and (d) 1400 °C, 1.5 h.

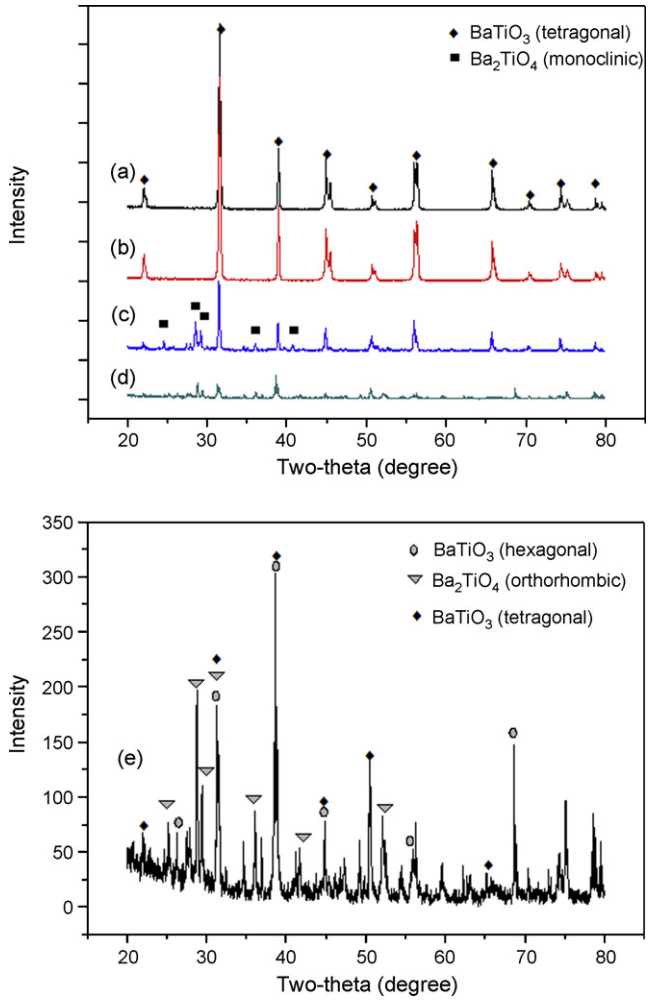

Fig. 9. X-ray diffraction patterns of BT sintered at different temperature: (a) 1300, (b) 1325, (c) 1350, (d) 1400, and (e) detail of (d).

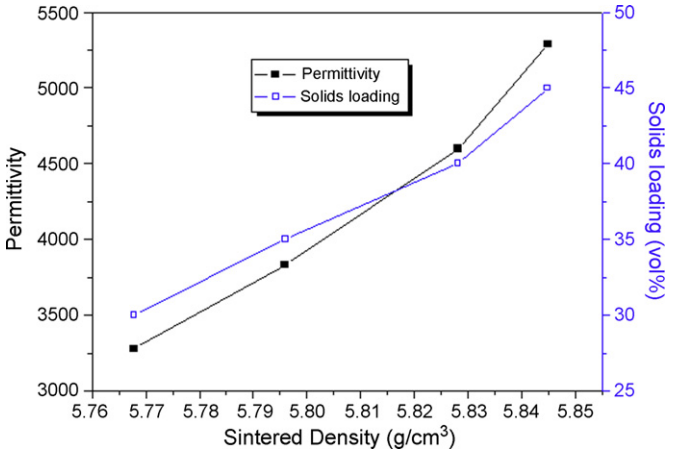

Fig. 10. Solids loading and room temperature dielectric constant (1 kHz) versus sintered density, samples sintered at optimal temperature (1325 °C, 1.5 h).

the sintering temperature was increased, the bulk density first increased, and then decreased. The permittivity showed a similar behaviour. Sintered at 1325 °C, the specimens gained the highest bulk density and relative permittivity. The cross-sectional SEM micrographs of the ceramics sintered at different temperatures are shown in Fig. 8. Samples sintered at 1300, 1325 °C present a uniform distribution of the grain sizes and their grain sizes increased as the sintering temperature increased. Abnormal coarse grains were found in the specimen sintered at 1350 °C. The grain structure was not apparent in the sample sintered at 1400 °C, indicating an even stronger overgrowth of the grains at such a sintering temperature. Moreover, all the sample sintered at 1350 and 1400 °C show more porosity compared with the sample sintered at 1325 °C, which could be one of the factors leading to the reduction in sintered density at this temperature.

The phase evolution of the sintered samples is shown in Fig. 9. The main phase found in samples sintered at 1300 and 1325 °C was tetragonal $BaTiO_3$ phase indicated by its strong peak splitting around $2\theta = 45°$. Tetragonal phase was still the main phase in the sample sintered at 1350 °C (Fig. 9(c)), however, the barium-rich titanate phase of Ba_2TiO_4 (monoclinic) was also found in this sample. In some work,[27] acid cleaning has been used to decrease the $BaCO_3$ content in commercial powders in order to limit the abnormal grain growth but this has not been done here. As mentioned in the powder characterization, impurity of $BaCO_3$ was found in this starting nano-sized BT powder, therefore, the barium-rich titanate phase of Ba_2TiO_4 could be formed through the reaction of BT with $BaCO_3$ in the powder at elevated temperature (1350 °C), consistent with Lu's work[22] as well. Furthermore, the theoretical density of monoclinic Ba_2TiO_4 is 5.20 g/cm^3 and less than that of tetragonal BT (6.02 g/cm^3), so the existence of Ba_2TiO_4 in this sample is another contributing factor to the decrease of sintered density. Seen from Fig. 9(d), the diffraction intensity of the sample sintered at 1400 °C weakened markedly compared with the samples sintered at lower temperatures (Fig. 9(a)–(c)), indicating poorer crystalline quality. Fig. 9(e) presents detailed patterns of this sample, which has been indexed using hexagonal BT and orthorhombic Ba_2TiO_4 phases. This is consistent with Ritter[28] who described that the orthorhombic phase was the high-temperature form of orthotitanate and the monoclinic one was stable at room temperature. In order to avoid excessive grain growth and these additional phases it can be concluded that 1325 °C is a suitable sintering temperature for this nano-BT powder.

Fig. 10 shows the initial solids loading and room temperature permittivity versus sintered density for samples sintered at 1325 °C for 1.5 h. When the solids loading is varied from 30 to 45 vol%, the sintered density changes from 5.77 g/cm^3 (95.8% of the theoretical density) to 5.85 g/cm^3 (97.0% of the theoretical density). The variation of the sintered density is only 1.2% of the theoretical density, which indicates that a good dispersion of this nano-sized BT powder has been achieved. As the sintered density increases, the relative permittivity of the bulk ceramic increases, whilst the loss tangent decreases from 0.037 to 0.01. Higher bulk density is helpful to improve electrical properties.

4. Conclusions

Rheological properties of suspensions with nano-sized BT powders have been characterized with regard to pH, solids loading and dispersant concentration. It is found that NH_4PAA is

very effective as a dispersant for this BT colloidal system. The pH value has strong effect on the stability of BT suspension, and moreover, the intrinsic pH is suitable for techniques such as centrifugal casting.

1325 °C is the optimal sintering temperature for this nano-sized BT powder. BT ceramic sintered at this temperature shows a bulk density of 5.85 g/cm^3, nearly 97.0% of the theoretical density, and room temperature dielectric constant and loss tangent as 5270 and 0.01, respectively.

Acknowledgments

The authors would like to thank the British Council and the University of Birmingham for the ORSAS award and research studentship. The authors are grateful to Mr. Carl Meggs for experimental assistance.

References

1. Kamiya, H., Gomi, K. and Iida, Y., Preparation of highly dispersed ultrafine barium titanate powder by using microbial-derived surfactant. *J. Am. Ceram. Soc.*, 2003, **86**(12), 2011–2018.
2. His, C.-S., Chen, Y.-C. and Jantunen, H., Barium titanate based dielectric sintered with a two-stage process. *J. Eur. Ceram. Soc.*, 2008, **28**, 2581–2588.
3. Russell, J. D. and Leach, C., β-Conductivity contrast at barium titanate thermistor grain boundaries. *J. Eur. Ceram. Soc.*, 1996, **16**, 1035–1039.
4. Liu, X., Luo, Y. and Li, X., Electrical properties of $BaTiO_3$-based NTC ceramics doped by $BaBiO_3$ and Y_2O_3. *J. Alloys Compd.*, 2008, **459**, 45–50.
5. Langhammer, H. T., Makovec, D. and Pu, Y., Grain boundary reoxidation of donor-doped barium titanate ceramics. *J. Eur. Ceram. Soc.*, 2006, **26**, 2899–2907.
6. Wang, X., Zhang, L. and Liu, H., Dielectric nonlinear properties of $BaTiO_3$–$CaTiO_3$–$SrTiO_3$ ceramics near the solubility limit. *Mater. Chem. Phys.*, 2008, **112**, 675–678.
7. Gomez-Yanez, C., Balmori-Ramirez, H. and Martinez, F., Colloidal processing of $BaTiO_3$ using ammonium polyacrylate as dispersant. *Ceram. Int.*, 2000, **26**, 609–616.
8. de Laat, A. W. M. and Derks, W. P. T., Colloidal stabilization of $BaTiO_3$ with poly (vinyl alcohol) in water. *Colloids Surf. A: Physicochem. Eng. Aspects*, 1993, **71**, 147–153.
9. de Laat, A. W. M. and van den Heuvel, G. L. T., Competitive and displacement adsorption of polyvinyl alcohol and the ammonium salt of a polyacrylic acid on $BaTiO_3$. *Colloids Surf. A: Physicochem. Eng. Aspects*, 1993, **70**, 179–187.
10. Blanco López, M. C., Fourlaris, G. and Riley, F. L., Interaction of barium titanate powders with an aqueous suspending medium. *J. Eur. Ceram. Soc.*, 1998, **18**, 2183–2192.
11. Blanco López, M. C., Rand, B. and Riley, F. L., Polymeric stabilisation of aqueous suspensions of barium titanate. Part II. Effect of polyelectrolyte concentration. *J. Eur. Ceram. Soc.*, 2000, **20**, 1587–1594.
12. Blanco López, M. C., Rand, B. and Riley, F. L., The isoelectric point of $BaTiO_3$. *J. Eur. Ceram. Soc.*, 2000, **20**, 107–118.
13. Blanco López, M. C., Rand, B. and Riley, F. L., The properties of aqueous phase suspensions of barium titanate. *J. Eur. Ceram. Soc.*, 1997, **17**, 281–287.
14. Li, C.-C. and Jean, J.-H., Interaction between dissolved Ba^{2+} and PAA-NH_4 dispersant in aqueous barium titanate suspensions. *J. Am. Ceram. Soc.*, 2002, **85**(6), 1449–1455.
15. Li, C.-C. and Jean, J.-H., Interaction of organic additives with boric oxide in aqueous barium titanate suspensions. *J. Am. Ceram. Soc.*, 2002, **85**(6), 1441–1448.
16. Zhao, J., Wang, X. and Li, L., Electrophoretic deposition of $BaTiO_3$ films from aqueous suspensions. *Mater. Chem. Phys.*, 2006, **99**, 350–353.
17. Mizuta, S., Parish, M. and Bowen, H. K., Dispersion of $BaTiO_3$ powders (Part I). *Ceram. Int.*, 1984, **10**, 43–48.
18. Bergstrom, L., Shinozaki, K., Tomiyama, H. and Mizutani, N., Colloidal processing of a very fine $BaTiO_3$ powder effect of particles on the suspension properties, consolidation and sintering behaviour. *J. Am. Ceram. Soc.*, 1997, **80**(2), 291–300.
19. Hirata, Y. and Kawabata, M., Dispersion and consolidation of ultrafine $BaTiO_3$ powder in non-aqueous solutions. *Mater. Lett.*, 1993, **16**, 175–180.
20. Hotta, Y., Tsunekawa, K. and Isobe, T., Synthesis of $BaTiO_3$ powders by a ball milling-assisted hydrothermal reaction. *Mater. Sci. Eng. A*, 2008, **475**, 12–16.
21. Jung, D. S., Hong, S. K. and Cho, J. S., Nano-sized barium titanate powders with tetragonal crystal structure prepared by flame spray pyrolysis. *J. Eur. Ceram. Soc.*, 2008, **28**, 109–115.
22. Lu, W., Quilitz, M. and Schmidt, H., Nanoscaled $BaTiO_3$ powders with a large surface area synthesized by precipitation from aqueous solutions: preparation, characterization and sintering. *J. Eur. Ceram. Soc.*, 2007, **27**, 3149–3159.
23. Kirby, G. H., Harris, D. J., Li, Q. and Lewis, J. A., Poly(acrylic acid)-poly(ethylene oxide) comb polymer effects on $BaTiO_3$ nanoparticles suspension stability. *J. Am. Ceram. Soc.*, 2004, **87**(2), 181–186.
24. Yu, J., Sun, X. and Li, Q., Preparation of Al_2O_3 and Al_2O_3–ZrO_2 ceramic foams with adjustable cell structure by centrifugal slip casting. *Mater. Sci. Eng. A*, 2008, **476**, 274–280.
25. Falamaki, C. and Veysizadeh, J., Taguchi design of experiments approach o the manufacture of one-step alumina microfilter/membrane supports by the centrifugal casting technique. *Ceram. Int.*, 2008, **34**, 1653–1659.
26. Zhang, D., Su, B. and Button, T. W., Preparation of concentrated aqueous alumina suspension for soft-molding microfabrication. *J. Eur. Ceram. Soc.*, 2004, **24**, 231–237.
27. Hérard, C., Faivre, A. and Lemí atre, J., Surface decontamination treatments of undoped $BaTiO_3$—Part: Powder and green body properties. *J. Eur. Ceram. Soc.*, 1995, **15**, 135–143.
28. Ritter, J. J., Roth, R. S. and Blendell, J. E., Alkoxide precursor synthesis and characterization of phases in the barium-titanium oxide system. *J. Am. Ceram. Soc.*, 1986, **69**(2), 155–162.